THE ADOPTION OF NOVEL COOLING LIQUIDS FOR ENHANCING HEAT TRANSFER PERFORMANCE OF THREE-DIMENSIONAL INTEGRATED CIRCUITS WITH EMBEDDED MICRO-CHANNEL

Huan HUANG[1], Chun SHAN[1], Futang LONG[1], Zongjie ZENG[1], Lei XIE[2], Fa ZOU[3], Peng XU[1*]

[*1] School of Electronics and Information, Guangdong Polytechnic Normal University, Guangzhou 510665, China.

[2] School of Food Science and Engineering, South China University of Technology, Guangzhou 510640, China.

[3] School of Electronics and Information Engineering, South China Normal University, Foshan 528225, China.

[*] Corresponding author; E-mail: xupeng@gpnu.edu.cn.

The nanofluids (including MWCNT based nanofluid and SWCNT based nanofluid) and liquid metal $Ga_{68}In_{20}Sn_{12}$ are proposed to replace the conventional water as cooling liquid of micro-channel for enhancing heat transfer performance of three-dimensional integrated circuits (3-D ICs) in this paper. An equivalent thermal model of 3-D ICs with integrated micro-channel is established to investigate the heat transfer performances for using different cooling liquids. The results show that the steady-state temperature for MWCNT based nanofluid, SWCNT based nanofluid and $Ga_{68}In_{20}Sn_{12}$ as cooling liquids can be reduced over 25.698%, 28.771% and 35.735% than the conventional water scheme in a four-layers stacked chip, respectively. Besides, it is found that the steady-state temperature of all die layer in 3-D ICs can be further reduced by increasing the micro-channel size and flow velocity of cooling liquid. Therefore, the proposed novel materials (i.e., nanofluids and $Ga_{68}In_{20}Sn_{12}$) as cooling liquids have excellent application prospect in solving thermal problems of 3-D ICs.

Key words*: three dimensional integrated circuits, micro-channel, heat transfer performance*

1. Introduction

The occurrence of three-dimensional (3-D) stacking technology has remarkably facilitated the progression of semiconductor integrated circuits, which extend the conventional two-dimensional integrated circuits (2-D ICs) entering into 3-D space [1]. Compared with 2-D ICs, 3-D ICs can reduce the total wire length, transmission delay, power dissipation and package size due to its multi-layer stacked structure in the vertical direction. However, the unique structure inevitably leads to the increase of power density of 3-D ICs, this can enable the 3-D ICs to form the complex thermal problem owing to the excessive temperature rise [2]. Hence, it is extremely vital that the chip designer ought to seek the solution for enhancing the heat transfer performance of 3-D ICs.

In recent years, the micro-channel cooling system has been widely used in high power semiconductor devices due to its excellent heat transfer performance [3–7]. Besides, it is recognized that the integration of micro-channel in 3-D ICs is regarded as an effective solution for solving the increasingly serious thermal problem. The micro-channel is embedded in the silicon substrate of each die layer and its interior is filled with cooling liquid. The cooling liquid convey the heat generated by back end of line (BEOL) to the external environment of 3-D ICs through heat conduction and convection [8]. Depending on the size of hydraulic diameter D_h, the micro-channel can be divided into nano-channel (i.e, D_h=10–1000 nm), micro-channel (i.e, D_h=1–100 μm), meso-channel (i.e, D_h=100–1000 μm) and macro-channel (i.e, D_h=1–6 mm), respectively [9, 10].

In the available literatures, water is the most common cooling liquid of micro-channel for practical application. However, the heat transfer performance of water as cooling liquid is limited in the light of its small thermal conductivity of 0.611 W/m·K [11]. Therefore, researchers are urgent to seek the novel materials with better heat transfer performance for replacing the conventional water as cooling liquid to solve the complex thermal problem of 3-D ICs due to the excessive temperature rise. Nanofluids have captured the intensive interest from many researchers that are composed of the ultra-fine nanoparticles (such as carbon nanotubes (CNTs) etc.) mixed in fluids (such as oil, water, engine oil etc.) in specific proportions [12–14]. The thermal properties of ultra-fine nanoparticles is far larger than water, which result in the thermal conductivity of nanofluids exceeding water [15, 16]. The CNTs are the cylindrical nanostructure of one or more graphene layers, which can be classified into single-wall carbon nanotubes (SWCNT) and multi-wall carbon nanotubes (MWCNT) depending on the number of carbon walls [17]. Based on the statement of Ref. [18], the diameters of SWCNT and MWCNT nanoparticles are commonly 0.8 to 2 nm, and 5 to 20 nm, respectively. In this work, the SWCNT and MWCNT are adopted as the ultra-fine nanoparticles because their thermal conductivity can reach to 6600 W/m·K and 3000 W/m·K, respectively [19]. In view of the small sizes and the large particular surface area of nanoparticles, the SWCNT and MWCNT based nanofluids have a series of excellent performance such as high thermal conductivity, less blockage in the transit of the fluid flow, longer stabilization and homogeneity [20]. Thus, the MWCNT based nanofluid and SWCNT based nanofluid as cooling liquids are investigated in our work. Besides the nanofluids, the liquid metals are also regarded as a promising potential cooling liquid in the research community in terms of their excellent heat transfer performance. $Ga_{68}In_{20}Sn_{12}$, composed of 68% gallium, 20% indium and 12% tin (calculating by weight), is deemed as the prospective cooling liquid of micro-channel [21]. The thermal conductivity of $Ga_{68}In_{20}Sn_{12}$ can exceed 39 W/m·K, which is far greater than the thermal conductivity of water (i.e., 0.6 W/m·K) under the same conditions [22, 23]. Therefore, the heat transfer performance for $Ga_{68}In_{20}Sn_{12}$ as cooling liquid of micro-channel in 3-D ICs is also discussed in this work.

In the practical applications, it is indispensable to investigate the preparation cost of different cooling liquids. The SWCNT and MWCNT nanoparticle powder are the essential materials for the preparation of nanofluids, and their price are usually 101 USD and 64 USD per gram, respectively [24]. Besides, the price of liquid metal $Ga_{68}In_{20}Sn_{12}$ is usually 0.38 USD per gram. Accordingly, the preparation cost for the proposed SWCNT based nanofluid, MWCNT based nanofluid and liquid metal $Ga_{68}In_{20}Sn_{12}$ as cooling liquids are much greater than the conventional water (usually 0.41 USD per ton in China) case [25]. Therefore, it is the key factor to reduce the preparation cost of these proposed cooling liquids for the future widespread application.

So far, there are some studies on improving heat transfer performance of micro-channel by replacing the conventional water with other promising cooling liquids that have been done. Abubakar *et al.* in Ref. [26] investigated the heat transfer performance of Fe_3O_4-H_2O as cooling liquid under four volume fractions (0, 0.4, 0.6, and 0.8), respectively. The results illustrated that increasing the volume fractions of nanofluids can improve the heat transfer performance of micro-channel. In Ref. [27], Kalteh established a numerical model to investigate the heat transfer performance of micro-channel for applying different types of nanofluid as cooling liquid cases in which nine different nanoparticles (i.e., Al_2O_3, CuO, Cu, Fe, Au, Ag, TiO_2, SiO_2 and diamond) are mixed in three different base fluid (i.e., water, ethylene glycol and engine oil) as nanofluids. The results shown that the diamond based nanofluid as cooling liquid of micro-channel has the highest heat transfer coefficient than other nanofluid. Sarafraz *et al.* in Ref. [28] studied the heat transfer performance of rectangular micro-channel for using the CNT based nanofluid and water as cooling liquids of micro-channel respectively, and the experimental results illustrated that the CNT based nanofluid as cooling fluid can effectively reduce the temperature of heat sink as compared with the conventional water case. Amrollahi *et al.* in Ref. [29] measured the heat transfer coefficients of MWCNT based nanofluid at horizontal tube, the results suggested that the convective heat transfer coefficients of MWCNT based nanofluid can be improved over 33% under the concentration of 0.25 wt.%, as compared with the pure water case. In Ref. [30], Liu *et al.* proposed the liquid metal GaInSn for replacing the conventional water as cooling liquid, which can enhance heat transfer performance of T-Y-type micro-channel evidently. Moreover, in Refs. [31–33], it is reported that $Ga_{68}In_{20}Sn_{12}$ as cooling liquid can efficiently improve the heat transfer performance of micro-channel in heat sink when compared with the pure water case.

Based on these discussions mentioned above, the conventional water is replaced with the nanofluids and $Ga_{68}In_{20}Sn_{12}$, which can obviously improve the heat transfer performance of micro-channel. However, at present few researches have investigated the nanofluids and liquid metal $Ga_{68}In_{20}Sn_{12}$ as cooling liquids of micro-channel for enhancing the heat transfer performance of 3-D ICs on the basis of the available literatures. In addition, till date most researches concerning 3-D ICs with integrated micro-channel are carried out by the COMSOL or ANSYS simulation, while the studies for proposing the numerical computation thermal model to quickly calculate temperature of 3-D ICs with integrated micro-channel are still rare. Meanwhile, it is widely known that the numerical computation model can evidently reduce the running time of CPU and memory consumption as compared with the COMSOL or ANSYS simulation. Therefore, a numerical computation thermal model of 3-D ICs with integrated micro-channel is proposed for rapid calculation of the temperature results of all die layer. Besides the conventional water, other potential cooling liquids including of nanofluids and liquid metal $Ga_{68}In_{20}Sn_{12}$ for using in 3-D ICs are also investigated in this paper. In order to verify the correctness of our proposed computational thermal model, thus its results are compared with the COMSOL simulation. The main contributions of this work are evaluated as below:

(1) The novel cooling liquids concerning SWCNT based nanofluid, MWCNT nanofluid and $Ga_{68}In_{20}Sn_{12}$ are proposed to replace the conventional water as cooling liquid of micro-channel for improving heat transfer performance of 3-D ICs.

(2) A computation thermal model is established in this work to improve operating efficiency of solving steady-state temperature of 3D-ICs with embedded micro-channel.

(3) The heat transfer performance of 3-D ICs can be improved by increasing the micro-channel size and flow velocity of cooling liquid.

2. Computational model

2.1. Modeling method

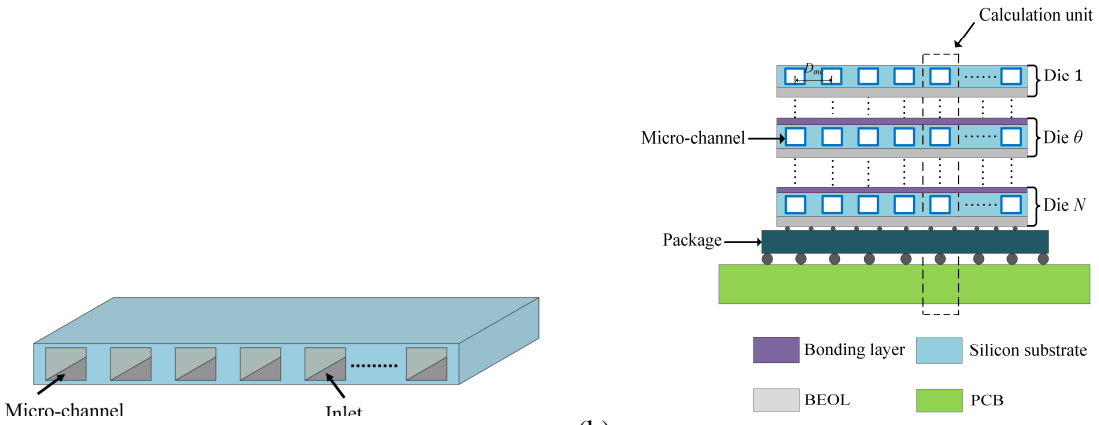

Fig. 1. The geometric structure diagrams: (a) 3-D view of micro-channel, (b) section view of *N*-layers stacked chip with embedded micro-channel.

The geometric structure diagram concerning micro-channel and 3-D ICs with embedded micro-channel are exhibited in Fig. 1, where the *N*-layers stacked chip includes package, back end of line (BEOL), silicon substrate, bonding layer and micro-channel. At present, the epoxy material is the most commonly used material as bonding layer of 3-D ICs owing to its low curing shrinkage and high thermostability. And the 3-D ICs is constructed on the printed circuit board (PCB). Especially, the BEOL is an essential part of 3-D ICs that contains transistor devices and metal wire. The heat is generated by BEOL that must be convey to the external ambient of chip in time. Additionally, it is assumed that the micro-channel is uniformly embedded in the center of silicon substrate with the same distance D_{mc} and each micro-channel has same geometric dimensions.

In this work, only a square structure unit of 3-D ICs as shown in Fig. 2 is discussed since the overall structure is configured as the symmetrical structure. Herein, L is the side length of calculation unit, and the cross-section area of calculation unit is $L \times L$, w and h are the width and height of the micro-channel, and Q_θ (θ = 1, 2, …, N) represents heat generated by θ^{th} die layer. Moreover, the boundary conditions and assumptions for the proposed computation model are listed as below:

(1) The ambient temperature and inlet temperature of micro-channel are fixed in the calculation process.

(2) The flow is considered as the steady and fully developed in each channel.

(3) All materials in 3-D ICs possess the homogeneous spatial structure, where their thermophysical parameters are isotropic.

(4) The total amount of heat generated by heat source is fixed, which is evenly distributed on the surface of BEOL.

The methodology for the proposed computation model is also listed as below:

Step 1: Derive the equivalent thermal resistance of PCB, package, BEOL, silicon substrate, bonding layer and micro-channel, respectively. Especially, the equivalent thermal resistance of micro-channel includes conduction thermal resistance, convection thermal resistance and thermal resistance of cooling liquid.

Step 2: Construct the equivalent thermal resistance network of the N-die stacked calculation unit with embedded micro-channel.

Step 3: Deduce the equations between the steady-state temperature, thermal resistance and heat flow.

Step 4: Establish the matrix equation of heat flow transmission based on the Step 3.

Step 5: Solve the matrix equation of heat flow transmission to obtain steady-state temperature of each die layer of 3D-ICs.

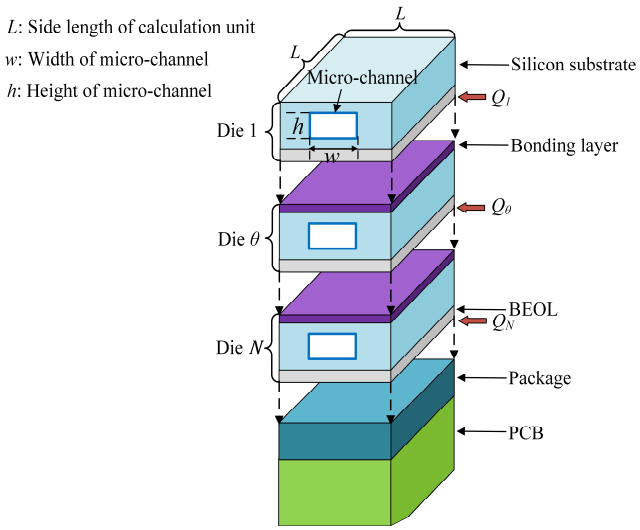

Fig. 2. The structure diagram of calculation unit.

2.2. Equivalent thermal model

According to the structure diagram of square unit shown in Fig. 2, we deduced a thermal resistance model of 3-D ICs with embedded micro-channel as depicted in Fig. 3 to represent the overall thermal characteristics of 3-D ICs. Herein R_{pcb} and R_{pk} denote the thermal resistance of PCB and thermal resistance of package for the calculation unit respectively. For the θ^{th} die layer (θ = 1, 2, …, N), $R_{BEOL,\theta}$ and $R_{bond,\theta}$ represent the thermal resistance of θ^{th} BEOL and bonding layer of calculation unit, respectively. $R_{con,\theta T}$, $R_{con,\theta B}$, $R_{con,\theta L}$ and $R_{con,\theta R}$ are the conduction thermal resistance of silicon substrate of calculation unit under top direction, bottom direction, left direction and right direction respectively. R_{conv} is the convection thermal resistance between solid and fluid, which is determined by physical parameters of micro-channel and cooling liquid. R_{cl} and $T_{BEOL,\theta}$ denote the thermal resistance of cooling liquid and the temperature of BEOL in θ^{th} die layer, respectively. $T_{mc,\theta T}$, $T_{mc,\theta B}$ are the temperature of top wall and bottom wall of micro-channel, respectively. $T_{out,\theta}$ and $T_{avg,\theta}$ represent outlet temperature of micro-channel and average temperature of cooling liquid for θ^{th} die layer, respectively.

For the calculation unit, the thermal resistance in vertical direction can be written as below [34],

$$R = \frac{t}{kA} \tag{1}$$

where, t and k are the thickness and thermal conductivity of materials, respectively. A is the cross-sectional area in the heat flow direction. According to equation (1) and Ref [2], R_{pcb}, R_{pk}, $R_{BEOL,\theta}$, $R_{con,\theta T}$, $R_{con,\theta B}$, $R_{con,\theta L}$, $R_{con,\theta R}$ and $R_{bond,\theta}$ (θ = 1, 2, …, N) can be derived as below,

$$R_{pcb} = \frac{t_{pcb}}{k_{pcb} L^2} \tag{2}$$

$$R_{pk} = \frac{t_{pk}}{k_{pk} L^2} \tag{3}$$

$$R_{BEOL,\theta} = \frac{t_{BEOL,\theta}}{k_{BEOL} L^2} \tag{4}$$

$$R_{con,\theta B} = R_{con,\theta T} = \frac{t_{si,\theta} - h}{2 k_{si} L^2} \tag{5}$$

$$R_{con,\theta L} = R_{con,\theta R} = \frac{2h}{k_{si}(L - w)L} \tag{6}$$

$$R_{bond,\theta} = \frac{t_{bond,\theta}}{k_{bond} L^2} \tag{7}$$

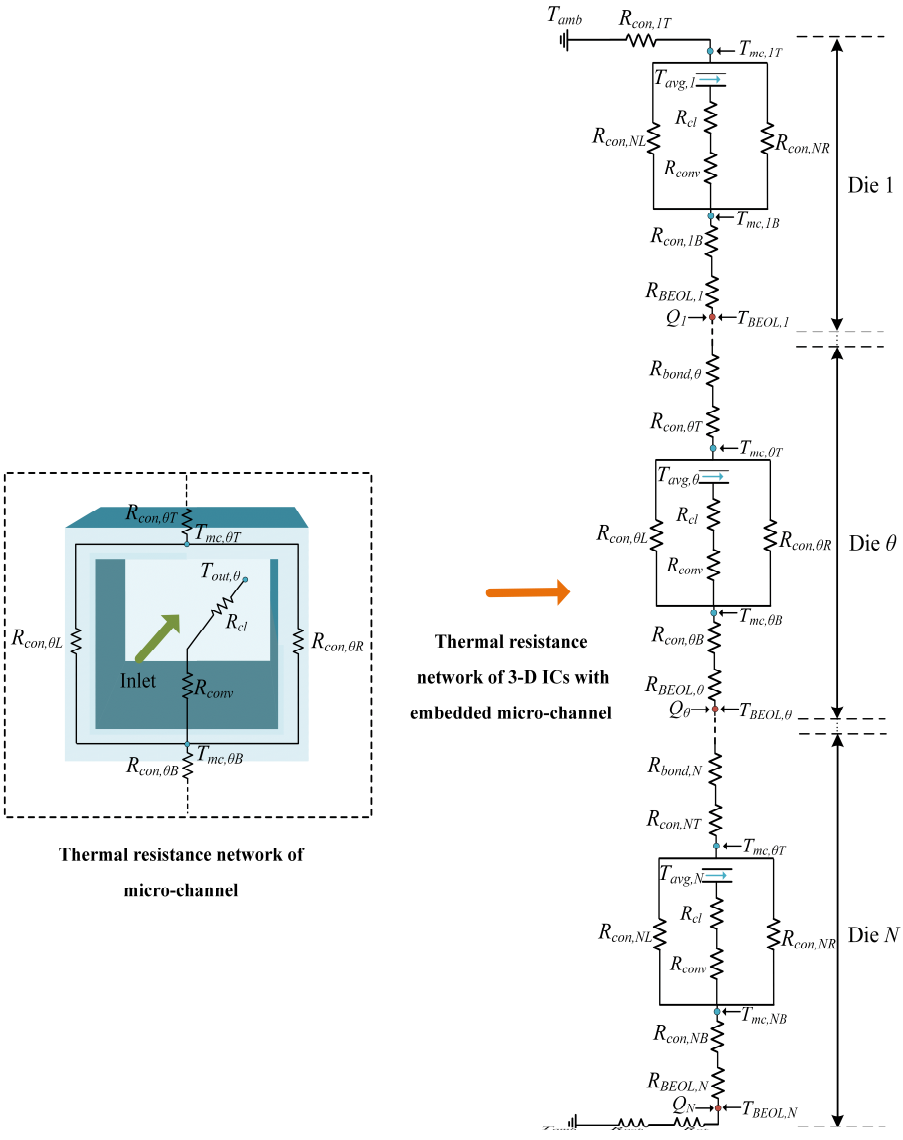

Fig. 3. The thermal resistance model of calculation unit.

Based on the Ref. [35], R_{conv} and R_{cl} can be deduced as,

$$R_{conv} = \frac{1}{h_{cl} A_m} \tag{8}$$

$$R_{cl} = \frac{1}{\rho_{cl} V_{cl} c_{cl}} \tag{9}$$

herein, ρ_{cl} and c_{cl} are the density and specific heat capacity of cooling liquid, respectively. h_{cl}, A_m and V_{cl} represent the convective heat transfer coefficient, heat transfer area and volume flow rate, which can be expressed as equation (10) to equation (12), respectively [36].

$$h_{cl} = \frac{Nuk_{cl}}{D_h} \tag{10}$$

$$A_m = wL + 2hL \tag{11}$$

$$V_{cl} = Uwh \tag{12}$$

here, k_{cl} and U denote the thermal conductivity and flow velocity of cooling liquid, respectively. According to the Ref. [37], the Nusselt number Nu and hydraulic diameter D_h are expressed as equation (13) and (14), respectively. Accordingly, the equation (13) can be used to derive the convective heat transfer coefficient in the light of equation (10).

$$Nu = 0.1165(\frac{D_h}{D_{mc}})^{0.81}(\frac{h}{w})^{-0.79} Re^{0.62} Pr^{1/3} \tag{13}$$

$$D_h = \frac{2wh}{(w+h)} \tag{14}$$

wherein, Re and Pr represent the Reynolds number and Prandtl number. Based on the Ref. [38], the corresponding expressions for them can be written as equations (15) and (16), respectively. Here, μ_{cl} is dynamic viscosity of cooling liquid.

$$Re = \frac{\rho_{cl} D_h U}{\mu_{cl}} \tag{15}$$

$$Pr = \frac{\mu_{cl} c_{cl}}{k_{cl}} \tag{16}$$

The relationship between temperature, thermal resistance and heat flow can be derived by using the Kirchhoff's Current Law (KCL) [39]. For the $\theta = N$ die layer, we can derive,

$$\frac{T_{BEOL,N} - T_{amb}}{R_{pk} + R_{pcb}} + \frac{T_{BEOL,N} - T_{mc,NB}}{R_{BEOL,N} + R_{con,NB}} = Q_N L^2 \tag{17}$$

$$\frac{T_{mc,NB} - T_{mc,NT}}{R_{con,NL}} + \frac{T_{mc,NB} - T_{avg,N}}{R_{conv} + R_{cl}} + \frac{T_{mc,NB} - T_{mc,NT}}{R_{con,NR}} = \frac{T_{BEOL,N} - T_{mc,NB}}{R_{BEOL,N} + R_{con,NB}} \tag{18}$$

$$\frac{T_{mc,NT} - T_{BEOL,(N-1)}}{R_{con,NT} + R_{bond,N}} = \frac{T_{mc,NB} - T_{mc,NT}}{R_{con,NL}} + \frac{T_{mc,NB} - T_{mc,NT}}{R_{con,NR}} \tag{19}$$

For the middle die layer ($\theta = N$ - 1, N - 2, …, 3, 2), we can deduce,

$$\frac{T_{BEOL,\theta} - T_{mc,\theta B}}{R_{BEOL,\theta} + R_{con,\theta B}} = Q_\theta L^2 + \frac{T_{mc,(\theta+1)T} - T_{BEOL,\theta}}{R_{con,(\theta+1)T} + R_{bond,(\theta+1)}} \tag{20}$$

$$\frac{T_{mc,\theta B} - T_{mc,\theta T}}{R_{con,\theta L}} + \frac{T_{mc,\theta B} - T_{avg,\theta}}{R_{conv} + R_{cl}} + \frac{T_{mc,\theta B} - T_{mc,\theta T}}{R_{con,\theta R}} = \frac{T_{BEOL,\theta} - T_{mc,\theta B}}{R_{BEOL,\theta} + R_{con,\theta B}} \tag{21}$$

$$\frac{T_{mc,\theta T}-T_{BEOL,(\theta-1)}}{R_{con,\theta T}+R_{bond,\theta}}=\frac{T_{mc,\theta B}-T_{mc,\theta T}}{R_{con,\theta L}}+\frac{T_{mc,\theta B}-T_{mc,\theta T}}{R_{con,\theta R}} \tag{22}$$

For the $\theta = 1$ die layer, we can solve,

$$\frac{T_{BEOL,1}-T_{mc,1B}}{R_{BEOL,1}+R_{con,1B}}=Q_1L^2+\frac{T_{mc,2T}-T_{BEOL,1}}{R_{con,2T}+R_{bond,2}} \tag{23}$$

$$\frac{T_{mc,1B}-T_{mc,1T}}{R_{con,1L}}+\frac{T_{mc,1B}-T_{avg,1}}{R_{conv}+R_{cl}}+\frac{T_{mc,1B}-T_{mc,1T}}{R_{con,1R}}=\frac{T_{BEOL,1}-T_{mc,1B}}{R_{BEOL,1}+R_{con,1B}} \tag{24}$$

$$\frac{T_{mc,1T}-T_{amb}}{R_{con,1T}}=\frac{T_{mc,1B}-T_{mc,1T}}{R_{con,1L}}+\frac{T_{mc,1B}-T_{mc,1T}}{R_{con,1R}} \tag{25}$$

The relationship between the temperature of bottom wall of micro-channel $T_{mc,\theta B}$, inlet temperature of micro-channel $T_{in,\theta}$ and outlet temperature of micro-channel $T_{out,\theta}$ can be given by equation (26) [40]. In addition, the average temperature of cooling liquid $T_{avg,\theta}$ can be defined by equation (27).

$$\ln\frac{T_{mc,\theta B}-T_{out,\theta}}{T_{mc,\theta B}-T_{in,\theta}}=-\frac{1}{R_{conv}R_{cl}} \tag{26}$$

$$T_{avg,\theta}=\frac{T_{in,\theta}+T_{out,\theta}}{2} \tag{27}$$

2.3. The relationship between pump power and flow velocity of cooling liquid

As the pump power is kept unchanged, the relationship between flow velocity of cooling liquid and geometric dimensions of micro-channel is mutual restraint. Both flow velocity of cooling liquid and geometric dimensions of micro-channel all can affect heat transfer performance of 3-D ICs. Hence, it is prominent to investigate the impacts of different micro-channel size on the heat transfer performance of 3-D ICs. Based on the Ref. [41], the relationship between flow velocity of cooling liquid and pump power can be given by,

$$U=D_h\sqrt{\frac{P_p}{2whnf\,\mathrm{Re}\,\mu_{cl}S}} \tag{28}$$

$$n=N\frac{S}{L} \tag{29}$$

$$f\,\mathrm{Re}=4.70+19.64\frac{\left(w^2+h^2\right)}{\left(w+h\right)^2} \tag{30}$$

where, the P_p, n, S and f are the pump power, number of channels, side length of chip and friction factor, respectively.

2.4. Thermophysical properties of nanofluids as cooling liquid

According to the Refs. [42, 43], the thermophysical parameters for MWCNT based nanofluid and SWCNT based nanofluid as cooling liquids of micro-channel can be obtained by the equations (31) - (34). Here the water is adopted as the carrier of nanofluids.

$$\rho_{nf}=\phi\rho_{np}+(1-\phi)\rho_{wt} \tag{31}$$

$$c_{nf} = \phi c_{np} + (1-\phi)c_{wt} \tag{32}$$

$$k_{nf} = \frac{1-\phi+\left(\frac{4\phi}{\pi}\right)\sqrt{\frac{k_{np}}{k_{wt}}}\text{arctg}\left(\frac{\pi}{4}\sqrt{\frac{k_{np}}{k_{wt}}}\right)}{1-\phi+\left(\frac{4\phi}{\pi}\right)\sqrt{\frac{k_{wt}}{k_{np}}}\text{arctg}\left(\frac{\pi}{4}\sqrt{\frac{k_{np}}{k_{wt}}}\right)}k_{wt} \tag{33}$$

$$\mu_{nf} = \frac{\mu_{wt}}{(1-\phi)^{2.5}} \tag{34}$$

here, $\emptyset$, ρ_{np}, c_{np} and k_{np} are volume fraction, density, specific heat capacity and thermal conductivity of nanoparticles, respectively. ρ_{wt}, c_{wt}, k_{wt} and μ_{wt} represent density, specific heat capacity, thermal conductivity and dynamic viscosity of water, respectively. ρ_{nf}, c_{nf}, k_{nf} and μ_{nf} denote density, specific heat capacity, thermal conductivity and dynamic viscosity of nanofluids, respectively.

2.5. Matrix equation of heat transfer in 3-D ICs

The equations from equations (17) - (25) contain $3N$ variables, which can be solved by the matrix equation as below,

$$FT = M \tag{35}$$

here, F is a $3N \times 3N$ multi-dimension sparse matrix that can be defined as,

$$F = \begin{bmatrix} \beta_1 & \beta_2 & 0 & 0 & 0 & 0 & 0 & \overbrace{0\cdots0}^{3N-7} \\ \beta_3 & \beta_4 & \beta_5 & 0 & 0 & 0 & 0 & \overbrace{0\cdots0}^{3N-7} \\ 0 & \beta_6 & \beta_7 & \beta_8 & 0 & 0 & 0 & \overbrace{0\cdots0}^{3N-7} \\ \vdots & \vdots & \vdots & \vdots & \vdots & \vdots & \vdots & \vdots \\ \overbrace{0\cdots0}^{3(N-\theta)-1} & \beta_9 & \beta_{10} & \beta_{11} & 0 & 0 & 0 & \overbrace{0\cdots0}^{3\theta-5} \\ \overbrace{0\cdots0}^{3(N-\theta)-1} & 0 & \beta_{12} & \beta_{13} & \beta_{14} & 0 & 0 & \overbrace{0\cdots0}^{3\theta-5} \\ \overbrace{0\cdots0}^{3(N-\theta)-1} & 0 & 0 & \beta_{15} & \beta_{16} & \beta_{17} & 0 & \overbrace{0\cdots0}^{3\theta-5} \\ \vdots & \vdots & \vdots & \vdots & \vdots & \vdots & \vdots & \vdots \\ \overbrace{0\cdots0}^{3N-7} & 0 & 0 & 0 & \beta_{18} & \beta_{19} & \beta_{20} & 0 \\ \overbrace{0\cdots0}^{3N-7} & 0 & 0 & 0 & 0 & \beta_{21} & \beta_{22} & \beta_{23} \\ \overbrace{0\cdots0}^{3N-7} & 0 & 0 & 0 & 0 & 0 & \beta_{24} & \beta_{25} \end{bmatrix} \tag{36}$$

wherein θ is in the range of 2 to (N - 1), and β_i (i = 1, 2, 3, …, 25) can be solved as below,

$$\beta_1 = \frac{1}{R_{PK} + R_{pcb}} + \frac{1}{R_{BEOL,N} + R_{con,NB}} \tag{37-1}$$

$$\beta_2 = \beta_3 = -\frac{1}{R_{BEOL,N} + R_{con,NB}} \tag{37-2}$$

$$\beta_4 = \frac{1}{R_{con,NL}} + \frac{1}{R_{conv} + R_{cl}} + \frac{1}{R_{con,NR}} + \frac{1}{R_{BEOL,N} + R_{con,NB}} \tag{37-3}$$

$$\beta_5 = \beta_6 = -\frac{1}{R_{con,NL}} - \frac{1}{R_{con,NR}} \tag{37-4}$$

$$\beta_7 = \frac{1}{R_{con,NT} + R_{bond,N}} + \frac{1}{R_{con,NL}} + \frac{1}{R_{con,NR}} \tag{37-5}$$

$$\beta_8 = -\frac{1}{R_{con,NT} + R_{bond,N}} \tag{37-6}$$

$$\beta_9 = -\frac{1}{R_{con,(\theta+1)T} + R_{bond,(\theta+1)}} \tag{37-7}$$

$$\beta_{10} = \frac{1}{R_{BEOL,\theta} + R_{con,\theta B}} + \frac{1}{R_{con,(\theta+1)T} + R_{bond,(\theta+1)}} \tag{37-8}$$

$$\beta_{11} = \beta_{12} = -\frac{1}{R_{BEOL,\theta} + R_{con,\theta B}} \tag{37-9}$$

$$\beta_{13} = \frac{1}{R_{con,\theta L}} + \frac{1}{R_{conv} + R_{cl}} + \frac{1}{R_{con,\theta R}} + \frac{1}{R_{BEOL,\theta} + R_{con,\theta B}} \tag{37-10}$$

$$\beta_{14} = \beta_{15} = -\frac{1}{R_{con,\theta L}} - \frac{1}{R_{con,\theta R}} \tag{37-11}$$

$$\beta_{16} = \frac{1}{R_{con,\theta T} + R_{bond,\theta}} + \frac{1}{R_{con,\theta L}} + \frac{1}{R_{con,\theta R}} \tag{37-12}$$

$$\beta_{17} = -\frac{1}{R_{con,\theta T} + R_{bond,\theta}} \tag{37-13}$$

$$\beta_{18} = -\frac{1}{R_{con,2T} + R_{bond,2}} \tag{37-14}$$

$$\beta_{19} = \frac{1}{R_{BEOL,1} + R_{con,1B}} + \frac{1}{R_{con,2T} + R_{bond,2}} \tag{37-15}$$

$$\beta_{20} = \beta_{21} = -\frac{1}{R_{BEOL,1} + R_{con,1B}} \tag{37-16}$$

$$\beta_{22} = \frac{1}{R_{con,1L}} + \frac{1}{R_{conv} + R_{cl}} + \frac{1}{R_{con,1R}} + \frac{1}{R_{BEOL,1} + R_{con,1B}} \tag{37-17}$$

$$\beta_{23} = \beta_{24} = -\frac{1}{R_{con,1L}} - \frac{1}{R_{con,1R}} \tag{37-18}$$

$$\beta_{25} = \frac{1}{R_{con,1T}} + \frac{1}{R_{con,1L}} + \frac{1}{R_{con,1R}} \tag{37-19}$$

The $3N \times 1$ matrix T represents the specific temperature of the stacked layer that can be expressed as below,

$$T = \begin{bmatrix} T_{BEOL,N} & T_{mc,NB} & T_{mc,NT} & \cdots & T_{BEOL,\theta} & T_{mc,\theta B} & T_{mc,\theta T} & \cdots & T_{BEOL,1} & T_{mc,1B} & T_{mc,1T} \end{bmatrix}^T \tag{38}$$

The M is also a $3N \times 1$ matrix, which is depended on the initial physical parameters of 3-D ICs, and its expression can be solved by,

$$M = \begin{bmatrix} Q_N L^2 + \frac{T_{amb}}{R_{pk} + R_{pcb}} & \frac{T_{avg,N}}{R_{conv} + R_{cl}} & 0 & \cdots & Q_\theta L^2 & \frac{T_{avg,\theta}}{R_{conv} + R_{cl}} & 0 & \cdots & Q_1 L^2 & \frac{T_{avg,1}}{R_{conv} + R_{cl}} & \frac{T_{amb}}{R_{con,1T}} \end{bmatrix}^T \tag{39}$$

3. Results and discussions

The heat transfer performance of 3-D ICs with embedded micro-channel for applying different cooling liquids (i.e., water, nanofluids and $Ga_{68}In_{20}Sn_{12}$) are studied in this section. The thermophysical property parameters of water, nanoparticles (i.e., SWCNT and MWCNT) and $Ga_{68}In_{20}Sn_{12}$ under ambient temperature are shown in Table 1 [42, 44, 45].

Table 1. The thermophysical property parameters of water, nanoparticles and $Ga_{68}In_{20}Sn_{12}$.

Materials	Density, (kg/m^3)	Specific heat capacity (J/kg·K)	Thermal conductivity (W/m·K)	Dynamic viscosity (Pa·S)
Water	996	4178	0.611	8.59×10^{-4}
MWCNT	1600	796	3000	-
SWCNT	2600	425	6600	-
$Ga_{68}In_{20}Sn_{12}$	6363.2	346.4	25.378	2.22×10^{-3}

In this work, the 3-D ICs is configured as a four-layers stacked chip, and the impacts of different micro-channel size on heat transfer performance of 3-D ICs are analyzed by utilizing our proposed computational thermal model. And all relevant physical and geometric parameters are shown in Table 2. Additionally, it is assumed that each die layer has same physical configuration, in the meantime each BEOL layer generates the same amount of heat. All the computation results of our proposed model are carried out by MATLAB R2020b. In order to ensure the correctness of our proposed model, where the computation results are validated against the COMSOL simulation and previous study (i.e., Ref. [46]), respectively. Here, the Ref. [46] has also proposed a numerical computation model to obtain steady-state temperature of 3-D ICs with integrated micro-channel. And our computer configuration for CPU and memory are the Intel i7-12650H and 32 GB, respectively.

Table 2. All relevant physical and geometric parameters of calculation unit.

Parameters	Values
Chip size ($S \times S$)	2000 μm × 2000 μm
Unit size ($L \times L$)	80 μm × 80 μm
Thickness and thermal conductivity of PCB (t_{pcb} and k_{pcb})	500 μm, 0.8 W/m·K
Thickness and thermal conductivity of package (t_{pk} and k_{pk})	200 μm, 4.1 W/m·K
Thickness and thermal conductivity of BEOL (t_{BEOL} and k_{BEOL})	10 μm, 1.4 W/m·K
Thickness and thermal conductivity of silicon substrate (t_{si} and k_{si})	60 μm, 130 W/m·K
Thickness and thermal conductivity of bonding layer (t_{bond} and k_{bond})	5 μm, 0.3 W/m·K
Width and height of micro-channel (w and h)	60 μm, 50 μm
Center distance of micro-channel (D_{mc})	80 μm
Heat generated by each die layer (Q)	1.25×10^6 W/m^2
Ambient temperature and inlet temperature of micro-channel (T_{amb} and $T_{in,\theta}$)	28 □

3.1. Heat transfer performance of novel cooling liquids

In this work, the specific temperature of each stacked die layer is calculated by utilizing our proposed computational thermal model, which take the different type of cooling liquids (i.e., water, nanofluids and liquid metal $Ga_{68}In_{20}Sn_{12}$) into account. Here, the micro-channel size is kept unchanged

and the flow velocity of cooling liquid is set as 1 m/s. In addition, the volume fraction of SWCNT and MWCNT as nanoparticles in nanofluid are all adopted as 0.03 [47].

3.1.1 Results of heat transfer performance for using different cooling liquids

The calculation temperature results of each BEOL die layer for water, nanofluids and $Ga_{68}In_{20}Sn_{12}$ as cooling liquids are listed in Table 3. As shown in Table 3, it is obvious that the nanofluids and $Ga_{68}In_{20}Sn_{12}$ as cooling liquids have lower temperature than the conventional water scheme for any stacked die layer. Meanwhile it is inferred from Table 3 that the $Ga_{68}In_{20}Sn_{12}$ as cooling liquid has the lowest temperature when compared with the other cooling liquids (i.e., water and nanofluids) for all stacked die layer. Using the θ = 3 die layer as an example, the temperature reduction for MWCNT based nanofluid, SWCNT based nanofluid and $Ga_{68}In_{20}Sn_{12}$ as cooling liquid schemes are exceeding 25.698%, 28.771% and 35.735% respectively, as compared with the conventional water scheme. Therefore, the nanofluids and liquid metal $Ga_{68}In_{20}Sn_{12}$ for substituting the traditional water as cooling liquids of micro-channel have excellent application prospect in enhancing the heat transfer performance of 3-D ICs.

Table 3. The temperature results of each BEOL layer for using different cooling liquids.

Type of cooling liquid	Temperature of BEOL layer, $T_{BEOL,\theta}$ (□)			
	$\theta = 1$	$\theta = 2$	$\theta = 3$	$\theta = 4$
Water	40.914	53.470	58.830	63.921
MWCNT based nanofluid	37.585	42.258	43.712	47.261
SWCNT based nanofluid	37.127	40.828	41.904	45.269
$Ga_{68}In_{20}Sn_{12}$	35.948	37.445	37.807	40.719

The simulation models for adopting the water, nanofluids and $Ga_{68}In_{20}Sn_{12}$ as cooling liquids of micro-channel are established to verify the accuracy of our proposed computational thermal model by utilizing COMOSL simulation in this work, respectively. The mesh type of our COMOSL simulation model is adopted as the tetrahedral division, where the general size of mesh elements is configured as "extremely fine", and the corresponding single die layer of calculation unit is shown in Fig. 4. Herein, the smallest element size is predefined in COMSOL simulation, which can guarantee the grid convergence. The COMSOL software utilized an iterative scheme to solve the governing partial differential equations, and the prescribed converging tolerance is 0.0001. The equations are solved iteratively behind till the individual values reach stability, or converge.

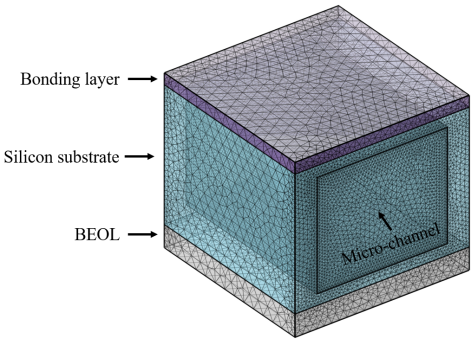

Fig. 4. The single die layer of calculation unit with embedded micro-channel for adopting the tetrahedral mesh with the extremely fine division.

In the simulation process of solving steady-state temperature, the governing equations of mass, momentum and energy can be listed as [48] below. The continuity equation for the fluid: $\nabla\cdot(\rho_{cl}U) = 0$. The momentum equation for the fluid: $(U\cdot\nabla)\rho_{cl}U = -\nabla p+\mu_{cl}\nabla^2U$. The energy equation for the fluid: $\rho_{cl}c_{cl}U\cdot\nabla T = k_{cl}\nabla^2T$. The energy equation for the solid: $k_s\nabla^2T = 0$. Here, p and k_s represent the pressure and thermal conductivity of solid, respectively.

The boundary condition and assumptions for COMSOL simulation model are listed as [49]:

(1) The heat transfer in solid and fluid module are coupled by using the non-isothermal flow feature.

(2) The micro-channel inlet boundary conditions are configured as uniform temperature T_{in} with a uniform flow velocity U.

(3) The flow is assumed to be steady and fully developed in each channel.

(4) The ambient temperature of physical field is adopted as T_{amb}.

(5) The top surface of $\theta = 1$ die layer and bottom surface of PCB of 3-D ICs are configured as natural convection, and other surfaces are set as adiabatic state.

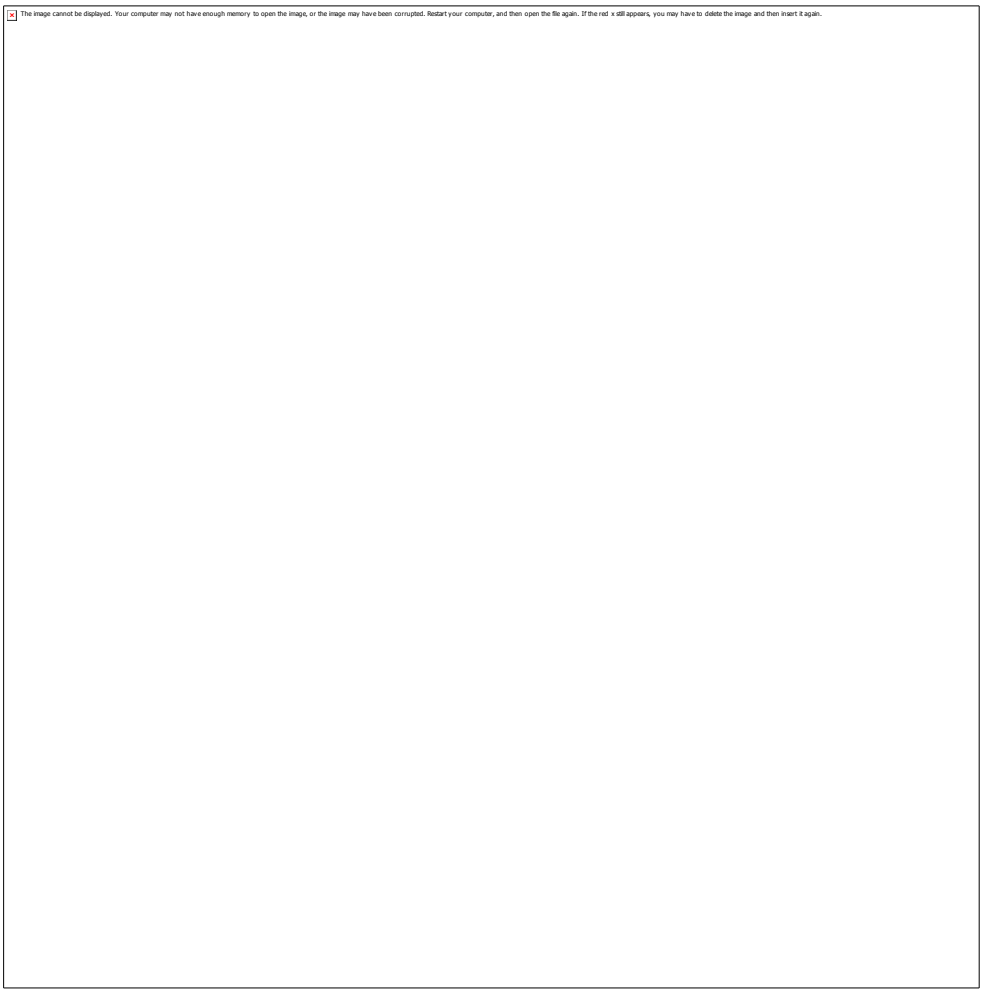

Fig. 5. The simulation temperature results of all BEOL die layer for using different cooling liquids: (a) water as cooling liquid, (b) MWCNT based nanofluid as cooling liquid, (c) SWCNT based nanofluid as cooling liquid, (d) $Ga_{68}In_{20}Sn_{12}$ as cooling liquid.

The corresponding temperature results of COMSOL simulation of all BEOL die layer for using different cooling liquids are exhibited in Fig. 5. Herein, the simulation temperature of each BEOL die

layer are obtained by the average steady-state temperature $T_{sr,avg}$. The $T_{sr,avg}$ is defined as $T_{sr,avg} = T_{sr,sum} / P_{sum}$, where $T_{sr,sum}$ represents the total temperature of all extracted points, and P_{sum} denotes the number of all extracted points. In addition, the points separated by 5 μm in the x, y and z directions on the BEOL die layer are selected as the extracted points, and the corresponding total extracted points are 867 in this work. Based on the analysis of results, it can be found that the conclusions obtained from Fig. 5 have close agreement with the Table 3.

Moreover, the comparison results for our proposed computational model and COMSOL simulation are shown in Fig. 6. In the meantime, the corresponding relative error results of all stacked die layer for them are depicted in Fig. 6. Where the relative error is defined as $\delta = |T_{cr} - T_{sr,avg}| / T_{sr,avg}$. Herein T_{cr} represents the temperature of our proposed computational model. Besides, in order to further ensure the accuracy of our proposed numerical computation model, their numerical results are validated with the numerical model of Ref. [46]. Meanwhile, the corresponding relative error results of all stacked die layer involved in them are also described in Fig. 6, and the relative error is expressed as $\delta_{ref} = |T_{cr} - T_{ref}| / T_{ref}$. Wherein T_{ref} denotes that the temperature results are obtained by the numerical model of Ref. [46].

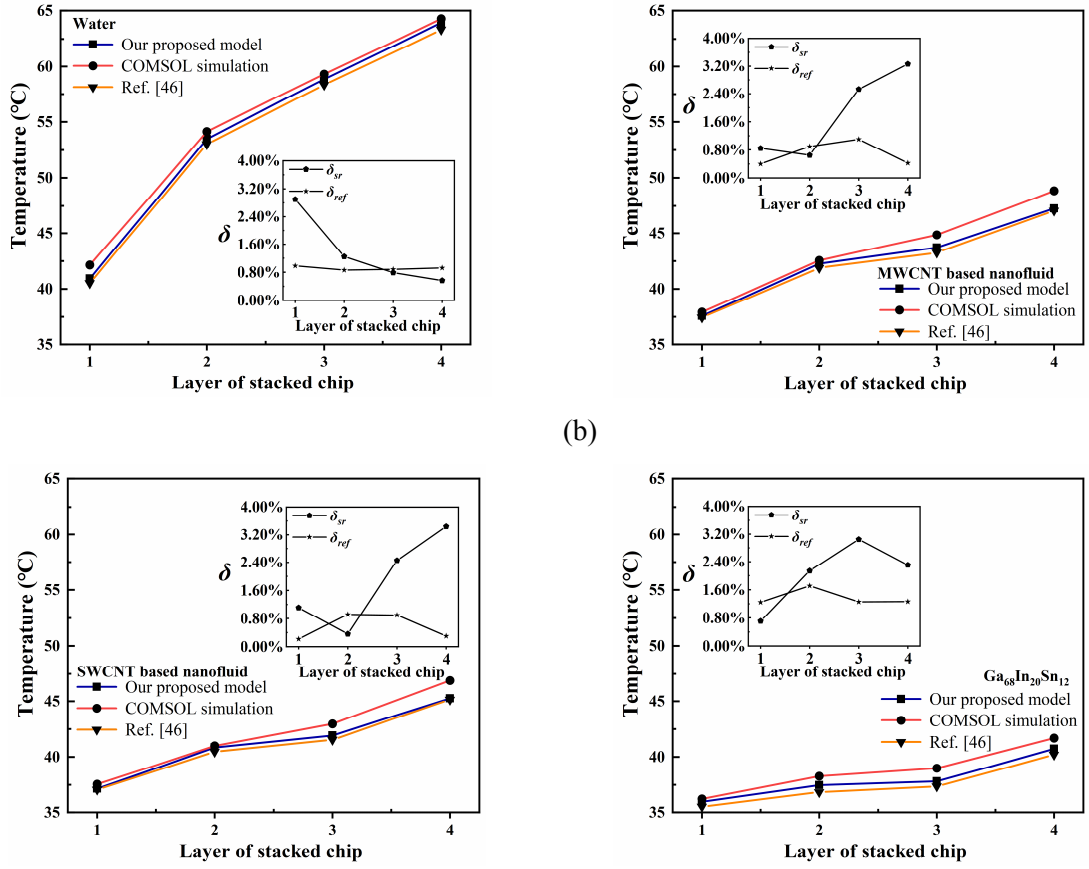

(a) (b)

(c) (d)

Fig. 6. The comparison results for our proposed computational thermal model, COMOSL simulation and the numerical model of Ref. [46]: (a) water as cooling liquid, (b) MWCNT based nanofluid as cooling liquid, (c) SWCNT based nanofluid as cooling liquid, (d) $Ga_{68}In_{20}Sn_{12}$ as cooling liquid.

From the displayed Fig. 6, it is evidently seen that the results of our proposed computation thermal model are fairly consistent with the COMOSL simulation results and the computation results of Ref. [46] in all cooling liquids, and the maximum relative error for them is less than 4%.

The differences of memory consumption and running time of CPU between our proposed numerical computation model, COMOSL simulation model and the numerical model of Ref. [46] are investigated in this section. The corresponding results of all cooling liquids for them are listed in Table 4, respectively.

As described in Table 4, it is remarkable that our proposed computation model can effectively reduce the memory consumption and running time of CPU as compared with the COMSOL simulation and the numerical model of Ref. [46]. Taking the $Ga_{68}In_{20}Sn_{12}$ as cooling liquid as an instance, the memory consumption of our proposed model can be reduced over 59.848% and 32.911% than the COMSOL simulation and Ref. [46], respectively, and the corresponding running time of CPU for them can be reduced over 86.547% and 63.943%, respectively. Consequently, our proposed computation thermal model can prominently reduce memory consumption and significantly improve CPU operating efficiency when compared with COMSOL simulation and the similar study (i.e., Ref. [46]).

Table 4. The memory consumption and running time of CPU for solving temperature results of different types of cooling liquids.

Working fluid type	Memory consumption and running time of CPU		
	Our proposed model	COMSOL simulation	Ref. [46]
Water	5.1 GB and 181 s	13.1 GB and 1479 s	7.8 GB and 547 s
MWCNT based nanofluid	5.2 GB and 196 s	13.3 GB and 1580 s	7.9 GB and 559 s
SWCNT based nanofluid	5.3 GB and 209 s	13.4 GB and 1588 s	8.0 GB and 584 s
$Ga_{68}In_{20}Sn_{12}$	5.3 GB and 203 s	13.2 GB and 1509 s	7.9 GB and 563 s

3.1.2 Discussions of thermophysical parameters for using different cooling liquid

In order to analyze the heat transfer performance for using different cooling liquid cases, the key thermophysical parameters concerning friction factor, rate of heat transfer, Nusselt number and flow velocity are investigated in this work when the range of pump power is from 0.02 to 0.05 W [50, 51]. The corresponding results are depicted in Fig. 7, respectively. Here, according to Newton's law of cooling, the rate of heat transfer for θ^{th} die layer can be defined as $\psi_\theta = A_m h_{cl}(T_{mc,\theta B} - T_{avg,\theta})$ [52]. The overall rate of heat transfer ψ_{ov} for all die layer of 3-D ICs can be expressed as $\psi_{eq} = \psi_1+\psi_2+\psi_3+\psi_4$.

As shown in Fig. 7(a), it can be seen that the friction factor of $Ga_{68}In_{20}Sn_{12}$ as cooling liquid is smaller than other cooling liquids. The reason behind this is that the kinematic viscosity ($= \mu_{cl} / \rho_{cl}$) of $Ga_{68}In_{20}Sn_{12}$ is much smaller than other cooling liquids, thus the $Ga_{68}In_{20}Sn_{12}$ as cooling liquid has a lower friction factor based on the equations (15) and (30).

As depicted in Fig. 7(b), the overall rate of heat transfer for MWCNT based nanofluid, SWCNT based nanofluid and $Ga_{68}In_{20}Sn_{12}$ as cooling liquid cases are larger than water as cooling liquid case. In the meantime, it can be observed from Fig. 7(b) that the $Ga_{68}In_{20}Sn_{12}$ as cooling liquid case has the largest overall rate of heat transfer as compared with other cooling liquid cases. This can be explained that the overall rate of heat transfer decreases with the increase of convection thermal resistance R_{conv} based on the aforementioned discussion and equation (8).

Based on the equations (13)-(16), the Nusselt number for all cooling liquids can be solved, which are exhibited in Fig. 7(c). The Fig. 7(c) shows that the Nusselt number of MWCNT based nanofluid, SWCNT based nanofluid and $Ga_{68}In_{20}Sn_{12}$ as cooling liquids are larger than the conventional water case, meanwhile the $Ga_{68}In_{20}Sn_{12}$ as cooling liquid has the largest Nusselt number in comparison with other cooling liquid cases. Besides, it can be seen from Fig.7(c) that the Nusselt number for all cooling liquids increases as the pump power increases. This is due to the fact that the flow velocity of cooling liquid increases with the increase of the pump power, thereby resulting in the increase of Reynolds number, then lead to the Nusselt number increase according to equations (13) and (15).

The results of Fig. 7(d) show that the flow velocity of water as cooling liquid is greater than other cooling liquids under the same pump power condition. The reason for this phenomenon is that the equivalent dynamic viscosity of water is smaller than other cooling liquids, and the flow velocity decreases as dynamic viscosity increases based on the equation (28).

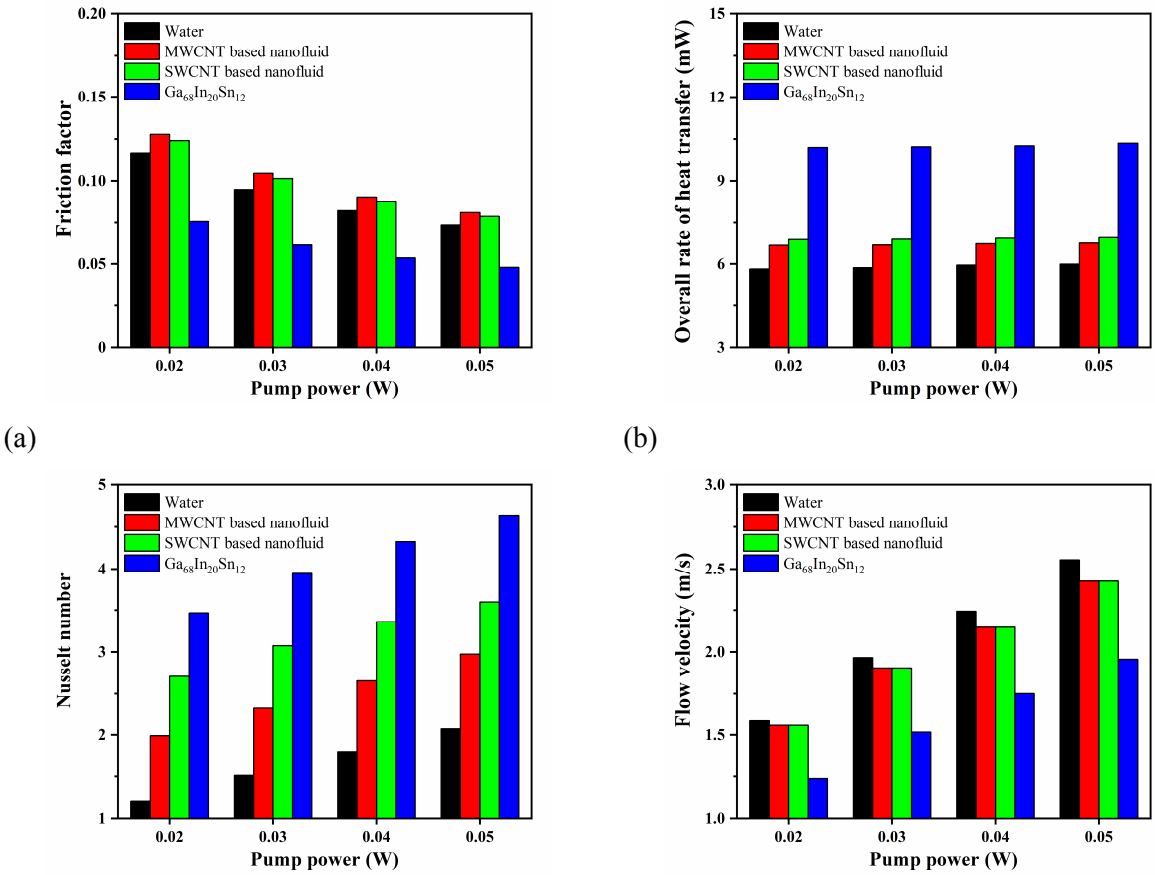

Fig. 7. The key thermophysical parameters with different pump power for using different cooling liquids: (a) friction factor, (b) overall rate of heat transfer, (c) Nusselt number (d) flow velocity.

3.1.3 Discussions of heat transfer performance for using different cooling liquid

Based on the results of this section, it is concluded that the steady-state temperature of all die layer for using the MWCNT based nanofluid, SWCNT based nanofluid and $Ga_{68}In_{20}Sn_{12}$ as cooling liquids are lower than the conventional water case. Meanwhile the steady-state temperature of all die

layer for the $Ga_{68}In_{20}Sn_{12}$ as cooling liquid is lower than other cooling liquids. The reason behind this is that the $Ga_{68}In_{20}Sn_{12}$ has the largest thermal conductivity as compared with other cooling liquids, in the meantime the water has the smallest thermal conductivity in comparison with other cooling liquids. Therefore, the $Ga_{68}In_{20}Sn_{12}$ and water as cooling liquids have the smallest and largest convection thermal resistance when compared with other cooling liquids based on equation (8) and (10). Consequently, the 3-D ICs with integrated micro-channel for the $Ga_{68}In_{20}Sn_{12}$ as cooling liquid has the lowest steady-state temperature as compared with the cases of MWCNT based nanofluid, SWCNT based nanofluid and water as cooling liquids. Certainly, the nanofluids and liquid metal $Ga_{68}In_{20}Sn_{12}$ can be regarded as an effective solution for substituting the traditional water as cooling liquid of micro-channel to enhance heat transfer performance of 3-D ICs in the future application.

In addition, it can be inferred that our proposed computation thermal model can obviously reduce memory consumption and running time of CPU when compared with COMSOL simulation. This can be explained that the COMSOL simulation software is implemented by a steady-state solver to calculate the temperature results, which is required to execute the steps for discrete grid and iterative calculations. There is no doubt that these steps need to spend more CPU execution time and memory consumption. However, the numerical computation model has no the steps of discrete grid and iterative calculation in the process of solving steady-state temperature.

3.2. Effects of micro-channel size on heat transfer performance of 3-D ICs

The flow velocity of cooling liquid and the contact area between the micro-channel and cooling liquid are determined by micro-channel size according to equations (11) (12) and (28), which can affect the value of convection thermal resistance and thermal resistance of cooling liquid. Hence, it is crucial to investigate the effects of micro-channel size on heat transfer performance of micro-channel. Therefore, the effects of micro-channel size on steady-state temperature of 3-D ICs are investigated in this section. Here, the pump power is fixed and its value is set as 0.05 W. And the $Ga_{68}In_{20}Sn_{12}$ is adopted as the cooling liquid of micro-channel in this section owing to its excellent heat transfer performance. Besides, the σ ($\sigma = w / L$) and φ ($\varphi = h / t_{si}$) are defined as the width ratio of micro-channel and height ratio of micro-channel, respectively. In addition, it is reported from Refs. [53, 54] that the ranges of width ratio σ of micro-channel and height ratio φ of micro-channel are all adopted as from 0.3 to 0.9.

3.2.1 Results for effects of micro-channel size on heat transfer performance of 3-D ICs

The calculation results concerning flow velocity of cooling liquid and the maximum temperature are exhibited in Fig. 8. As depicted Fig. 8(a), it is found that the maximum and minimum flow velocity of cooling liquid are 1.969 m/s (i.e., when $\sigma = 0.7$ and $\varphi = 0.9$) and 1.413 m/s (i.e., when $\sigma = 0.9$ and $\varphi = 0.3$) under different micro-channel size, respectively. Consequently, the effects of geometry size of micro-channel on the flow velocity of cooling liquid ought to be taken into consideration when the pump power is fixed. In order to further investigate the impacts of micro-channel size on the temperature of 3-D ICs, the corresponding calculation results regarding the maximum temperature of four-layers stacked chip versus the micro-channel size are presented in Fig. 8(b). Here, the pump power is still kept unchanged. As shown in Fig. 8(b), it is suggested that the maximum temperature of all die layer occurs its lowest value of 38.650 □ when the micro-channel size reach to its maximum value (i.e., the maximum micro-channel size with σ =0.9 and φ=0.9).

Meanwhile, it can be inferred that the maximum temperature of all die layer for the maximum micro-channel size case (i.e., σ = 0.9 and φ = 0.9) can be reduced over 19.351% than the minimum micro-channel size case (i.e., σ = 0.3 and φ = 0.3). Apparently, expanding the micro-channel size can significantly improve the heat transfer performance of 3-D ICs as the pump power is fixed.

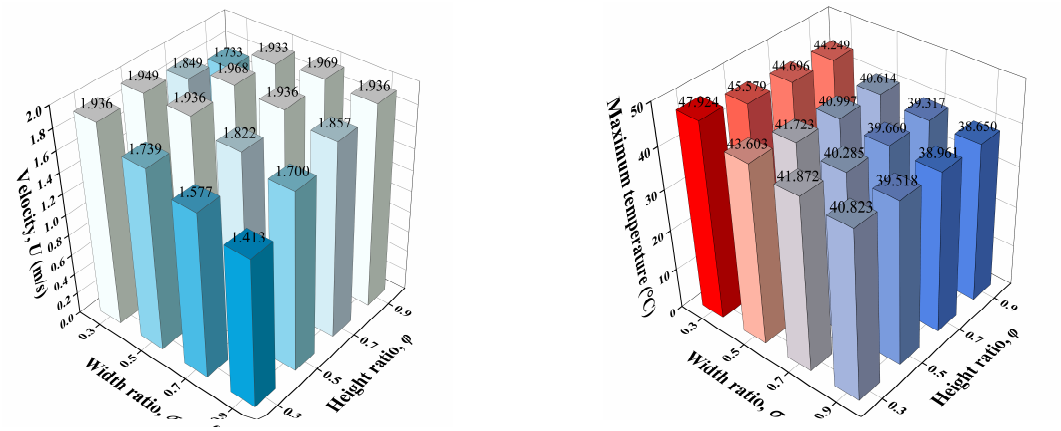

(a) (b)

Fig. 8. The calculation results concerning (a) flow velocity of cooling liquid versus micro-channel size and (b) the maximum temperature of 3-D ICs versus micro-channel size.

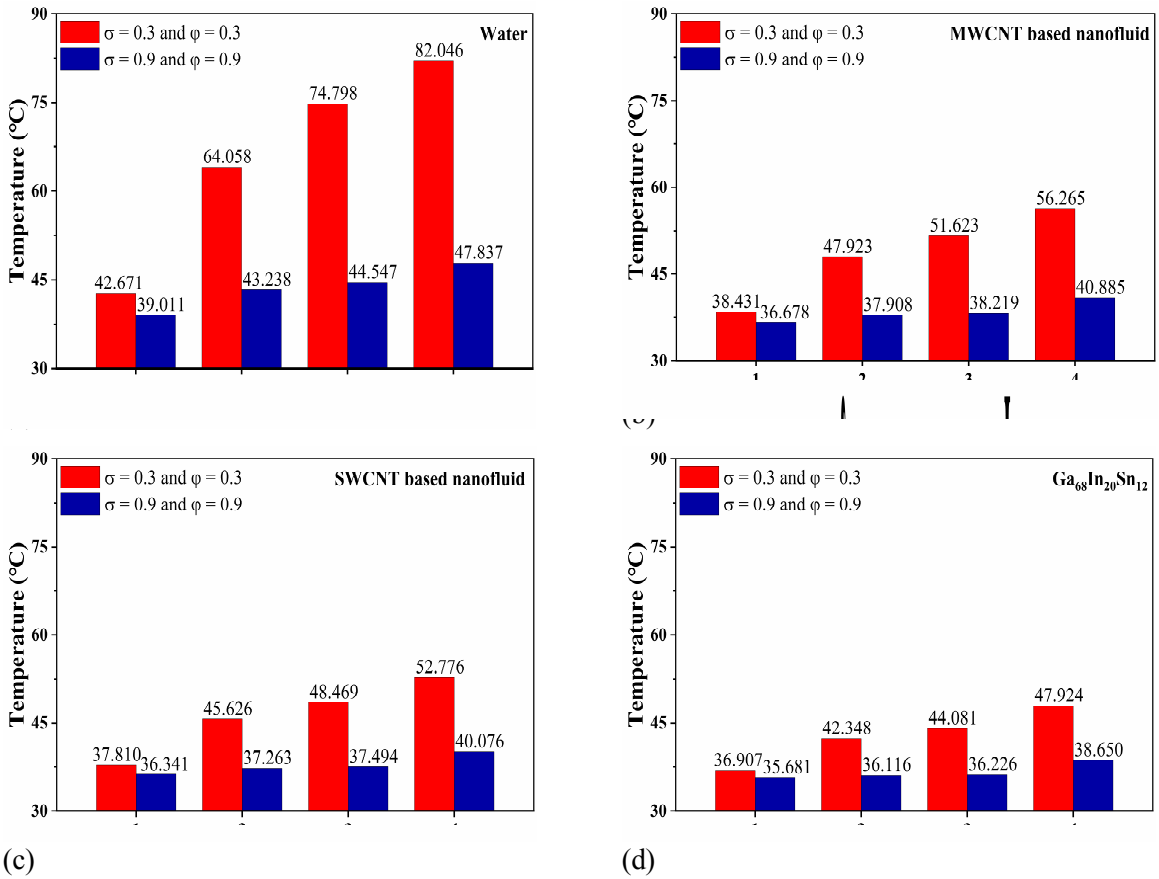

(c) (d)

Fig. 9. The specific temperature of each die layer of 3-D ICs for applying different type of cooling liquids under the maximum micro-channel size and the minimum micro-channel size: (a) water as cooling liquid, (b) MWCNT based nanofluid as cooling liquid, (c) SWCNT based nanofluid as cooling liquid, (d) $Ga_{68}In_{20}Sn_{12}$ as cooling liquid.

The heat transfer performance of different type of cooling liquids under the maximum micro-channel size (i.e., $\sigma = 0.9$ and $\varphi = 0.9$) and the minimum micro-channel size (i.e., $\sigma = 0.3$ and $\varphi = 0.3$) are investigated, and the corresponding temperature results are displayed in Fig. 9.

As described in Fig. 9, it is implied that the temperature of each die layer can be obviously reduced by expanding the micro-channel size when the pump power is fixed. Using the $\theta = 4$ die layer as an example, the temperature for water, MWCNT based nanofluid, SWCNT based nanofluid and $Ga_{68}In_{20}Sn_{12}$ under the maximum micro-channel size case are reduced by 41.695%, 27.335%, 24.064% and 19.351% than the minimum micro-channel size case, respectively. Besides, it can be concluded from Fig. 9 that the heat transfer performance of nanofluids and $Ga_{68}In_{20}Sn_{12}$ as cooling liquids is still better than the conventional water as cooling liquid scheme. Taking the $\theta = 3$ die layer as an example, the reduction percentages of temperature for MWCNT based nanofluid, SWCNT based nanofluid and $Ga_{68}In_{20}Sn_{12}$ as cooling liquids under the maximum micro-channel size scheme are exceeding 14.533%, 16.224% and 19.205% respectively, as compared with the conventional water scheme. Apparently, the nanofluids and liquid metal $Ga_{68}In_{20}Sn_{12}$ can be applied as the promising cooling liquids of micro-channel for enhancing heat transfer performance of 3-D ICs.

3.2.2 Discussions for effects of micro-channel size on heat transfer performance of 3-D ICs

According to the results of this section, it can be deduced that the heat transfer performance of 3-D ICs can be effectively enhanced by expanding the micro-channel size. This is due to the fact that the convective thermal resistance and thermal resistance of cooling liquid decrease with the increase of micro-channel size, thereby reducing the steady-state temperature. Besides, it is demonstrated that the nanofluids and $Ga_{68}In_{20}Sn_{12}$ as cooling liquids under the maximum micro-channel size scheme still have better heat transfer performance in comparison with the conventional water as cooling liquid. This can be explained that the nanofluids and $Ga_{68}In_{20}Sn_{12}$ as cooling liquids possess a lower convection thermal resistance as compared with the traditional water case on the basis of the aforementioned discussions. Therefore, expanding the micro-channel size can be seemed as a prospective method for enhancing heat transfer performance of 3-D ICs.

3.3. Effects flow velocity of cooling liquid on heat transfer performance of 3-D ICs

The effects of flow velocity of cooling liquid on heat transfer performance of 3-D ICs are investigated for this section. In order to obtain the different flow velocity of cooling liquid, the pump power is no longer kept unchanged. Here, the geometric dimensions of micro-channel are set as the maximum micro-channel size with $\sigma = 0.9$ and $\varphi = 0.9$, and the $Ga_{68}In_{20}Sn_{12}$ is selected as the cooling liquid of micro-channel.

3.3.1 Results for effects flow velocity of cooling liquid on heat transfer performance of 3-D ICs

The temperature results versus flow velocity of cooling liquid are shown in Table 5. As illustrated in Table 5, it is indicated that the temperature of all die layer decreases with the increase of flow velocity of cooling liquid. For instance, the temperature reduction for the die layer $\theta = 2$ can exceed 2.5 □ when the flow velocity of cooling liquid increases from 0.5 m/s to 2 m/s. Besides, it is also found that the pump power also increases as the flow velocity of cooling liquid increases. As an

instance, the pump power is increased over 17 times as the flow velocity of cooling liquid increases from 0.5 m/s to 2 m/s.

Table 5. The temperature results of 3-D ICs under different flow velocity of cooling liquid.

Flow velocity of cooling liquid	Pump power	Temperature of BEOL layer, $T_{BEOL,\theta}$ (□)			
		$\theta = 1$	$\theta = 2$	$\theta = 3$	$\theta = 4$
0.5 m/s	0.003 W	37.050	38.662	39.080	41.841
1 m/s	0.013 W	36.217	37.035	37.239	39.791
1.5 m/s	0.030 W	35.863	36.416	36.555	39.022
2 m/s	0.053 W	35.660	36.081	36.188	38.607

3.3.2 Discussions for effects flow velocity of cooling liquid on heat transfer performance of 3-D ICs

According to the results of Table 5, it can be implied that the heat transfer performance of 3-D ICs can be further improved by increasing the flow velocity of cooling liquids. The reason behind this is that the volume flow rate increases as the flow velocity of cooling liquid increases, then lead to the decrease of thermal resistance of cooling liquid combining of equations (9) and (12). Meanwhile, the power consumption of the pump will increase as the flow velocity of cooling liquid increases based on equation (28). Therefore, the constraint relationship between the pump power and the flow velocity of cooling liquid ought to be considered in the thermal design of 3-D ICs.

4. Conclusions

This paper proposed the novel cooling liquids (i.e., MWCNT based nanofluids, SWCNT based nanofluid and liquid metal $Ga_{68}In_{20}Sn_{12}$) for replacing the conventional water to enhance heat transfer performance of 3-D ICs with integrated micro-channel. In order to quickly obtain the steady-state temperature of 3-D ICs for using different types of cooling liquids, the corresponding numerical thermal model is established. Moreover, the effects of micro-channel size and flow velocity of cooling liquid on heat transfer performance of 3-D ICs are investigated by using our proposed computation model in this work. The main findings of this work are listed as follows:

(1) The reduction of steady-state temperature for MWCNT based nanofluid, SWCNT based nanofluid and $Ga_{68}In_{20}Sn_{12}$ as cooling liquid cases are exceeding 25.698%, 28.771% and 35.735% respectively, as compared with the conventional water case.

(2) Expanding the micro-channel size can be regarded as an effective method to improve heat transfer performance of 3-D ICs. The steady-state temperature for water, MWCNT based nanofluid, SWCNT based nanofluid and $Ga_{68}In_{20}Sn_{12}$ as cooling liquid cases can be reduced by 41.695%, 27.335%, 24.064% and 19.351% when the width ratio and height ratio of micro-channel increase from 0.3 to 0.9.

(3) The steady-state temperature of 3-D ICs decreases with the increase of flow velocity of cooling liquid. Meanwhile the pump power will increase as the flow velocity of cooling liquid increases.

(4) The results of our proposed computation thermal model have close agreement with the results of COMSOL simulation, and the maximum relative error involved in them is not exceeding 4%. In the

meantime, the memory consumption and running time of CPU for our proposed computation thermal model can be reduced over 59.848% and 86.547% than COMSOL simulation, respectively.

In the light of the presented results in this paper, it can be expected that the proposed new technology for utilizing the nanofluids and liquid metal $Ga_{68}In_{20}Sn_{12}$ as cooling liquids can be as an emerging technology to improve the heat transfer performance of 3-D ICs.

Nomenclature

Abbreviation			
BEOL	Back end of line	V_{cl}	Volume flow rate, [m^3s^{-1}]
CNTs	Carbon nanotubes	w	Width of micro-channel, [m]
MWCNT	Multi-wall carbon nanotubes	*Greek Symbols*	
PCB	Printed circuit board	β	Matrix elements
SWCNT	Single-wall carbon nanotubes	δ	Relative error
		μ	Dynamic viscosity [Pas]
English Symbols		ρ	Density [kgm^{-3}]
A	Cross-sectional area, [m^2]	ϕ	Volume concentration
A_m	Heat transfer area, [m^2]	ψ	Heat transfer rate [mW]
c	Specific heat capacity, [$Jkg^{-1}K^{-1}$]		
D_h	Hydraulic diameter, [m]	*Subscripts*	
D_{mc}	Distance of each micro-channel, [m]	amb	Ambient
f	Friction factor, [-]	avg	Average
h	Height of micro-channel, [m]	bond	Bonding layer of 3D-ICs
h_{cl}	Heat transfer coefficient, [$Wm^{-2}K^{-1}$]	cl	Cooling liquid
k	Thermal conductivity, [$Wm^{-1}K^{-1}$]	con	Conduction
L	Side length of calculation unit, [m]	conv	Convection
n	Number of channels, [-]	cr	Calculation results
Nu	Nusselt number, [-]	in	Inlet
P_p	Pump power. [W]	nf	Nanofluid
Pr	Prandtl number, [-]	np	Nanoparticles
Q	Heat generated, [Wm^{-2}]	out	Outlet
R	Thermal resistance, [KW^{-1}]	pk	Package of 3D-ICs
S	Side length of chip, [m]	ref	Reference
T	Temperature, [□]	sr	Simulation results
t	Thickness, [m]	wt	Water
U	Flow velocity, [ms^{-1}]		

Acknowledgment

This work was supported by National Natural Science Foundation of China (Grant No. 62273108), National Key Research and Development Program (Grant No. 2022YFB3604502), Youth Project of Guangdong Artificial Intelligence and Digital Economy Laboratory (Grant No. PZL2022KF0006), Major Science and Technology Project of Guangzhou Key Field R&D Plan (Grant No. 202206070001), Special Fund Project of Guangzhou Science and Technology Innovation Development (Grant No. 202201011307), Guangdong Provincial Department of Education Key

Construction Project (Grant No. 99166990222), Special Projects in Key Fields of General Colleges and Universities in Guangdong Province (Grant No. 2021ZDZX1016), Youth Project of Guangdong Province Basic and Applied Basic Research Fund (Grant No. 2023A1515110076), Guangzhou Basic Research Program (Grant No. 202201011286) and Scientific Research Startup Project of Guangdong Polytechnic Normal University (Grant No. 2021SDKYA032).

References

[1] Xu, P., Pan, Z.-L., Thermal Model for 3-D Integrated Circuits with Integrated MLGNR-Based Through Silicon Via, *Therm sci*, *24* (2020), 3 Part B, pp. 2067-2075

[2] Huang, H., et al., The Integration of Double-Layer Triangular Micro-Channel in Three-Dimensional Integrated Circuits for Enhancing Heat Transfer Performance, *Case Studies in Thermal Engineering*, *58* (2024), 104363

[3] Rikitu, E.H., Makinde, O.D., Entropy Generation and Heat Transfer Analysis of Eyring-Powell Nanofluid Flow Through Inclined Microchannel Subjected to Magnetohydrodynamics and Heat Generation, *International Journal of Thermofluids*, *22* (2024), 100640

[4] Makinde, O.D., Makinde, A.E., Thermal Analysis of a Reactive Variable Viscosity TiO_2-PAO Nanolubricant in a Microchannel Poiseuille Flow, *Micromachines*, *14* (2023), 6, pp. 1164

[5] Sindhu, S., et al., Hybrid Nanoliquid Flow Through a Microchannel with Particle Shape Factor, Slip and Convective Regime, *HFF*, *32* (2022), 10, pp. 3388-3410

[6] Kefene, M.Z., et al., MHD Variable Viscosity Mixed Convection of Nanofluid in a Microchannel with Permeable Walls, *IJPAP*, *58* (2020), 12, pp. 892-908

[7] Monaledi, R.L., Makinde, O.D., Entropy Generation Analysis in a Microchannel Poiseuille Flows of Nanofluid with Nanoparticles Injection and Variable Properties, *J Therm Anal Calorim*, *143* (2021), 3, pp. 1855-1865

[8] Huang, J.-H., et al., Experimental Study on Thermosyphon Boiling in 3-D Micro-Channels, *International Journal of Heat and Mass Transfer*, *131* (2019), pp. 1260-1269

[9] Shimizu, H., et al., Sensitive Determination of Concentration of Nonfluorescent Species in an Extended-Nano Channel by Differential Interference Contrast Thermal Lens Microscope, *Anal. Chem.*, *82* (2010), 17, pp. 7479-7484

[10] Fan, Y., Luo, L., Recent Applications of Advances in Microchannel Heat Exchangers and Multi-Scale Design Optimization, *Heat Transfer Engineering*, *29* (2008), 5, pp. 461-474

[11] Buongiorno, J., et al., A Benchmark Study on the Thermal Conductivity of Nanofluids, *Journal of Applied Physics*, *106* (2009), 9, 094312

[12] Zeeshan, A., et al., Computational Intelligence Approach for Optimising MHD Casson Ternary Hybrid Nanofluid over the Shrinking Sheet with the Effects of Radiation, *Applied Sciences*, *13* (2023), 17, 9510

[13] Zeeshan, A., et al., Electromagnetic Flow of SWCNT/MWCNT Suspensions in Two Immiscible Water- and Engine-Oil-Based Newtonian Fluids Through Porous Media, *Symmetry*, *14* (2022), 2, 406

[14] Ellahi, R., The Effects of MHD and Temperature Dependent Viscosity on the Flow of Non-Newtonian Nanofluid in a Pipe: Analytical Solutions, *Applied Mathematical Modelling*, *37* (2013), 3, pp. 1451-1467

[15] Zeeshan, A., et al., Mixed Convection Flow and Heat Transfer in Ferromagnetic Fluid over a Stretching Sheet with Partial Slip Effects, *Therm sci*, *22* (2018), 6 Part A, pp. 2515-2526

[16] Ellahi, R., et al., A Study of Heat Transfer in Power Law Nanofluid, *Therm sci*, *20* (2016), 6, pp. 2015-2026
[17] Pradhan, N.R., et al., The Specific Heat and Effective Thermal Conductivity of Composites Containing Single-Wall and Multi-Wall Carbon Nanotubes, *Nanotechnology*, *20* (2009), 24, 245705
[18] Ahmad, S., et al., Radiative SWCNT and MWCNT Nanofluid Flow of Falkner–Skan Problem with Double Stratification, *Physica A: Statistical Mechanics and its Applications*, *547* (2020), 124054
[19] Berber, S., et al., Unusually High Thermal Conductivity of Carbon Nanotubes, *Phys. Rev. Lett.*, *84* (2000), 20, pp. 4613-4616
[20] Nasrin, R., Alim, M.A., Free Convective Flow of Nanofluid Having Two Nanoparticles Inside a Complicated Cavity, *International Journal of Heat and Mass Transfer*, *63* (2013), pp. 191-198
[21] Hodes, M., et al., On the Potential of Galinstan-Based Minichannel and Minigap Cooling, *IEEE Trans. Compon., Packag. Manufact. Technol.*, *4* (2014), 1, pp. 46-56
[22] Muhammad, A., et al., Comparison of Pressure Drop and Heat Transfer Performance for Liquid Metal Cooled Mini-Channel with Different Coolants and Heat Sink Materials, *J Therm Anal Calorim*, *141* (2020), 1, pp. 289-300
[23] Yang, X.-H., et al., Flow and Thermal Modeling and Optimization of Micro/Mini-Channel Heat Sink, *Applied Thermal Engineering*, *117* (2017), pp. 289-296
[24] Yazid, M.N.A.W.M., et al., Heat and Mass Transfer Characteristics of Carbon Nanotube Nanofluids: A Review, *Renewable and Sustainable Energy Reviews*, *80* (2017), pp. 914-941
[25] Deng, Y., Liu, J., Design of Practical Liquid Metal Cooling Device for Heat Dissipation of High Performance CPUs, *Journal of Electronic Packaging*, *132* (2010), 3, 031009
[26] Abubakar, S.B., Sidik, N.A.C., Numerical Prediction of Laminar Nanofluid Flow in Rectangular Microchannel Heat Sink, *Journal of Advanced Research in Fluid Mechanics and Thermal Sciences*, *7* (2015), 1, pp. 29-38
[27] Kalteh, M., Investigating the Effect of Various Nanoparticle and Base Liquid Types on the Nanofluids Heat and Fluid Flow in a Microchannel, *Applied Mathematical Modelling*, *37* (2013), 18-19, pp. 8600-8609
[28] Sarafraz, M.M., et al., Fouling Formation and Thermal Performance of Aqueous Carbon Nanotube Nanofluid in a Heat Sink with Rectangular Parallel Microchannel, *Applied Thermal Engineering*, *123* (2017), pp. 29-39
[29] Amrollahi, A., et al., Convection Heat Transfer of Functionalized MWNT in Aqueous Fluids in Laminar and Turbulent Flow at the Entrance Region, *International Communications in Heat and Mass Transfer*, *37* (2010), 6, pp. 717-723
[30] Liu, H.-L., et al., Heat Transfer Performance of T-Y Type Micro-Channel Heat Sink with Liquid GaInSn Coolant, *International Journal of Thermal Sciences*, *120* (2017), pp. 203-219
[31] Tawk, M., et al., Numerical study of a liquid metal mini-channel cooler for power semiconductor devices, *Proceedings*, 2011 17th International Workshop on Thermal Investigations of ICs and Systems (THERMINIC), September 2011, pp. 1-6
[32] Liu, C., He, Z., High Heat Flux Thermal Management Through Liquid Metal Driven with Electromagnetic Induction Pump, *Front. Energy*, *16* (2022), 3, pp. 460-470
[33] Zhang, M., et al., Flow and Thermal Modeling of Liquid Metal in Expanded Microchannel Heat Sink, *Front. Energy*, (2023), *17* (2023), pp. 796–810

[34] Liu, Z., et al., Compact Lateral Thermal Resistance Model of TSVs for Fast Finite-Difference Based Thermal Analysis of 3-D Stacked ICs, *IEEE Trans. Comput.-Aided Des. Integr. Circuits Syst.*, *33* (2014), 10, pp. 1490-1502
[35] Baodong, S., et al., Multi□objective Optimization Design of a Micro□channel Heat Sink Using Adaptive Genetic Algorithm, *International Journal of Numerical Methods for Heat & Fluid Flow*, *21* (2011), 3, pp. 353-364
[36] Shi, B., Srivastava, A., Optimized Micro-Channel Design for Stacked 3-D-ICs, *IEEE Trans. Comput.-Aided Des. Integr. Circuits Syst.*, *33* (2014), 1, pp. 90-100
[37] Arshad, W., Ali, H.M., Experimental Investigation of Heat Transfer and Pressure Drop in a Straight Minichannel Heat Sink Using TiO_2 Nanofluid, *International Journal of Heat and Mass Transfer*, *110* (2017), pp. 248-256
[38] Kumar, R., Mahulikar, S.P., Effect of Temperature-Dependent Viscosity Variation on Fully Developed Laminar Microconvective Flow, *International Journal of Thermal Sciences*, *98* (2015), pp. 179-191
[39] Xu, P., et al., Thermal Performance Analysis of Carbon Materials Based TSV in Three Dimensional Integrated Circuits, *IEEE Access*, *11* (2023), pp. 75285-75294
[40] Çengel, Y.A., *Heat and Mass Transfer: A Practical Approach*, McGraw-Hill, Boston, 2007
[41] Husain, A., Kim, K.-Y., Design Optimization of Micro-Channel for Micro Electronic Cooling, *Proceedings*, ASME 5th International Conference on Nanochannels, Microchannels, and Minichannels, Puebla, Mexico, January 1, 2007, pp. 201-207
[42] Xia, G.D., et al., The Characteristics of Convective Heat Transfer in Microchannel Heat Sinks Using Al_2O_3 and TiO_2 Nanofluids, *International Communications in Heat and Mass Transfer*, *76* (2016), pp. 256-264
[43] Xue, Q.Z., Model for Thermal Conductivity of Carbon Nanotube-Based Composites, *Physica B: Condensed Matter*, *368* (2005), 1-4, pp. 302-307
[44] Hayat, T., et al., Melting Heat Transfer in Stagnation Point Flow of Carbon Nanotubes Towards Variable Thickness Surface, *AIP Advances*, *6* (2016), 1, pp. 015214
[45] Zhang, X.-D., et al., Experimental Investigation of Galinstan Based Minichannel Cooling for High Heat Flux and Large Heat Power Thermal Management, *Energy Conversion and Management*, *185* (2019), pp. 248-258
[46] Mizunuma, H., et al., Thermal Modeling and Analysis for 3-D ICs with Integrated Microchannel Cooling, *IEEE Trans. Comput.-Aided Des. Integr. Circuits Syst.*, *30* (2011), 9, pp. 1293-1306
[47] Nimmagadda, R., Venkatasubbaiah, K., Two-Phase Analysis on The Conjugate Heat Transfer Performance of Microchannel with Cu, Al, SWCNT, And Hybrid Nanofluids, *Journal of Thermal Science and Engineering Applications*, *9* (2017), 4, 041011
[48] Gong, L., et al., Thermal Management and Structural Parameters Optimization of MCM-BGA 3D Package Model, *International Journal of Thermal Sciences*, *147* (2020), 106120
[49] Scognamillo, C., et al., Numerical Analysis of the Thermal Impact of Ceramic Materials in Double-Sided Cooled Power Modules, *Proceedings*, 2020 26th International Workshop on Thermal Investigations of ICs and Systems (THERMINIC), Berlin, Germany, September 14, 2020, pp. 1-5
[50] Vasilev, M.P., et al., Effect of Microchannel Heat Sink Configuration on The Thermal Performance and Pumping Power, *International Journal of Heat and Mass Transfer*, *141* (2019), pp. 845-854

[51] Choudhury, B.K., Gouda, M.K., CFD Analysis of Heat Transfer in Liquid-Cooled Heat Sink For Different Microchannel Flow Field Configuration, in: *Advances in Air Conditioning and Refrigeration* (Eds. M. Ramgopal et al.), Springer Singapore, Singapore, 2021, pp. 381-393
[52] Wang, H., et al., Influence of Geometric Parameters on Flow and Heat Transfer Performance of Micro-Channel Heat Sinks, *Applied Thermal Engineering*, *107* (2016), pp. 870-879
[53] Lim, S.K., *Design for High Performance, Low Power, and Reliable 3D Integrated Circuits*, Springer New York, New York, NY, 2013
[54] Ohadi, M., et al., *Next Generation Microchannel Heat Exchangers*, Springer New York, New York, NY, 2013

Submitted: 14.04.2024.
Revised: 20.05.2024.
Accepted: 26.05.2024.